

Article

CO₂ Transfer Characteristics of Calcareous Humid Subtropical Forest Soils and Associated Contributions to Carbon Source and Sink in Guilin, Southwest China

Fen Huang ^{1,2}, Jianhua Cao ^{1,2,*}, Tongbin Zhu ^{1,2}, Mingzhu Fan ^{1,2} and Mengmeng Ren ^{1,3}

¹ Key Laboratory of Karst Dynamics, Institute of Karst Geology (CAGS), Ministry of Natural Resources (MNR) and Guangxi, Guilin 541004, China; hfen@karst.ac.cn (F.H.); zhutongbin@gmail.com (T.Z.); fanmingzhu3071@163.com (M.F.); luckdevin@163.com (M.R.)

² International Research Center on Karst, Under the Auspices of United Nations Educational, Scientific and Cultural Organization (UNESCO), Guilin 541004, China

³ School of Water Resources and Environment, China University of Geosciences (Beijing), Beijing 100083, China

* Correspondence: jhcaogl@163.com; Tel.: +86-773-779-6626

Received: 4 January 2020; Accepted: 11 February 2020; Published: 14 February 2020



Abstract: In karst landscapes, soil CO₂ is a key factor in weathering processes and carbon cycling, where its distribution and migration characteristics directly affect fluxes in carbon source–sink dynamics. We measured the CO₂ emission and dissolution rates of carbonate tablets in calcareous soil developed from limestone and red soil developed from clastic rock, in karst and non-karst subtropical forests, in Guilin, southwest China between 2015 and 2018, to analyze their CO₂ transfer characteristics and source–sink effects. The results showed similar average soil respiration rates between calcareous soil and red soil, with an average CO₂ emission flux of 1305 and 1167 t C km^{−2} a^{−1}, respectively. Carbonate tablet dissolution rates were bidirectional with increasing depth and were greater in red soil than calcareous soil, averaging 13.88 ± 5.42 and 7.20 ± 2.11 mg cm^{−2} a^{−1}, respectively. CO₂ concentration was bidirectional with increasing soil depth, reaching a maximum at the base of the soil–atmosphere interface (50–60 cm), and the bidirectional gradient was more distinctive in red soil. Change in the carbon isotope value of soil CO₂ was also bidirectional in calcareous soils, for which the overall average was 0.87‰ heavier in calcareous than red soil. The carbon sink in calcareous soil in karst regions was estimated to be 11.97 times that of red soil in non-karst regions, whereas its role as a carbon source is just 1.12 times that of red soil, thus indicating the key role of karst soil in the reduction of atmospheric CO₂.

Keywords: subtropical forest; calcareous soils; red soils; soil CO₂; carbon source–sink

1. Introduction

As the largest carbon pool of the terrestrial ecosystem, the amount of total carbon stored in soil (2300 Pg) is about two times and three times higher than the amount stored in the atmosphere (750 Pg) and in living biomass (650 Pg), respectively [1]. Global soil CO₂ emission rates are now up to approximately 98 ± 12 Pg a^{−1}, which is an order of magnitude greater than total annual CO₂ emissions from human activities (6.8 Pg a^{−1}); thus, small fluctuations in soil CO₂ emissions can greatly affect concentrations of atmospheric CO₂ [2,3].

Notably, soil CO₂ is soluble in water and readily forms carbonic acid, which can react with some types of bedrock (e.g., carbonate rock) to consume soil CO₂ and act as an important carbon sink of

atmospheric CO₂ [4]. China has a karst area of 3.44 million km² [5], and the net recovery of atmospheric CO₂ from the weathering of carbonate rocks (karstification) can reach 36 million t C a⁻¹ [6], accounting for 48% of China's forest carbon sink (75 million t C a⁻¹) [7] between 1981 and 2000. The karst area of eight provinces in southwest China totals 1.12 million km², of which the bare karst area, depicted as carbonate rock exposed to the atmosphere directly, is 460,000 km² [5].

According to previous studies, the karstification that occurred in the soil–rock interface has affected the carbon isotope value ($\delta^{13}\text{C}$) of CO₂ from soil respiration and its distribution in the soil profile [8–12]. The CO₂ concentration in the limestone soil profile has a bidirectional gradient, with CO₂ concentration peaks typical in the middle layer [8–11]. In contrast, the CO₂ concentration in the red soil profile has a unidirectional gradient; that is to say, the deeper the red soil layer, the higher the CO₂ concentration [9]. However, unidirectional gradients with depth have also been recorded from 60 cm depths in limestone and dolomite soil profiles [12]. In the non-karst soil profile, the bidirectional gradient of CO₂ distribution was also reported [13,14]. The CO₂ concentration and amount of CO₂ emitted from soil respiration in limestone soil are both lower in karst areas than those of red soil in non-karst areas [9]. The $\delta^{13}\text{C}$ value of CO₂ from soil respiration in the karst area is 4‰ heavier than that of the non-karst area [9]. This difference may be related to consumption and absorption of soil CO₂ in the carbonate rock dissolution at the soil–rock interface of karst regions [9]. In the soil–atmosphere interface layer, the $\delta^{13}\text{C}$ value of soil CO₂ ($\delta^{13}\text{C}\text{-CO}_2$) decreased with an increase in soil depth; whereas, below the soil–atmosphere interface layer, the $\delta^{13}\text{C}\text{-CO}_2$ is basically unchanged in a karst soil [15].

Analysis of the $\delta^{13}\text{C}$ may be used to explore the source of CO₂ in soil. If the karstification effect is sufficiently large enough to influence soil CO₂ concentration distribution, it should first arouse the CO₂ isotope's response to the soil profiles, because the CO₂ dissociated from bicarbonate formed by karstification is one of the sources of the soil CO₂ in karst areas [12]. Therefore, to understand how it may affect $\delta^{13}\text{C}\text{-CO}_2$ and the release of CO₂, and evaluate the CO₂ source and sink effect of karst soils, we determined the CO₂ concentration and isotope value in three calcareous soil profiles, developed from limestone found in a subtropical forest, for three years, for which red soils developed from clastic rock of the same zone were chosen for comparison. The source of CO₂ emission in calcareous soil was collected by the chamber method, and the sink produced by karstification was calculated by the standard carbonate tablet method.

2. Materials and Methods

2.1. Study Site

The study area was located near Maocun village, about 30 km southeast of Guilin (110°30'00"–110°33'45" E, 25°10'11"–25°12'30" N), in a typical karst peak cluster depression and valley landscape, with a catchment of about 10 km² (Figure 1). The climate in the area is mid-subtropical humid monsoon, hot and humid summer, characterized by spatio-temporal variations in rainfall; the annual average temperature is 19.64–20.39 °C, and the annual average rainfall is 1160–1378 mm (Figure S1). The geology of karst areas consists of Upper Devonian Rongxian Formation (D_{3r}) pure limestone. Vegetation in the studied sites was comprised of an evergreen broad-leaved forest dominated by *Cyclobalanopsis glauca*, *Loropetalum chinense*, *Alchornea trewioides*, and *Nephrolepis auriculata*, whose soil type was brown calcareous soil of the primosol order in the genetic soil classification of China (GSCC) [16], with a depth of 0.2–1 m. The geology of non-karst areas comprises iron clastic rock (D₂¹). Vegetation in this studied site was comprised of an evergreen broad-leaved forest, dominated by *Castanopsis fargesii*, *Schima superba*, *Itea chinensis*, and a small amount of *Miscanthus* spp.; the soil type was red soil of the ferrallosol order in GSCC [16], with a depth of >1 m [9].

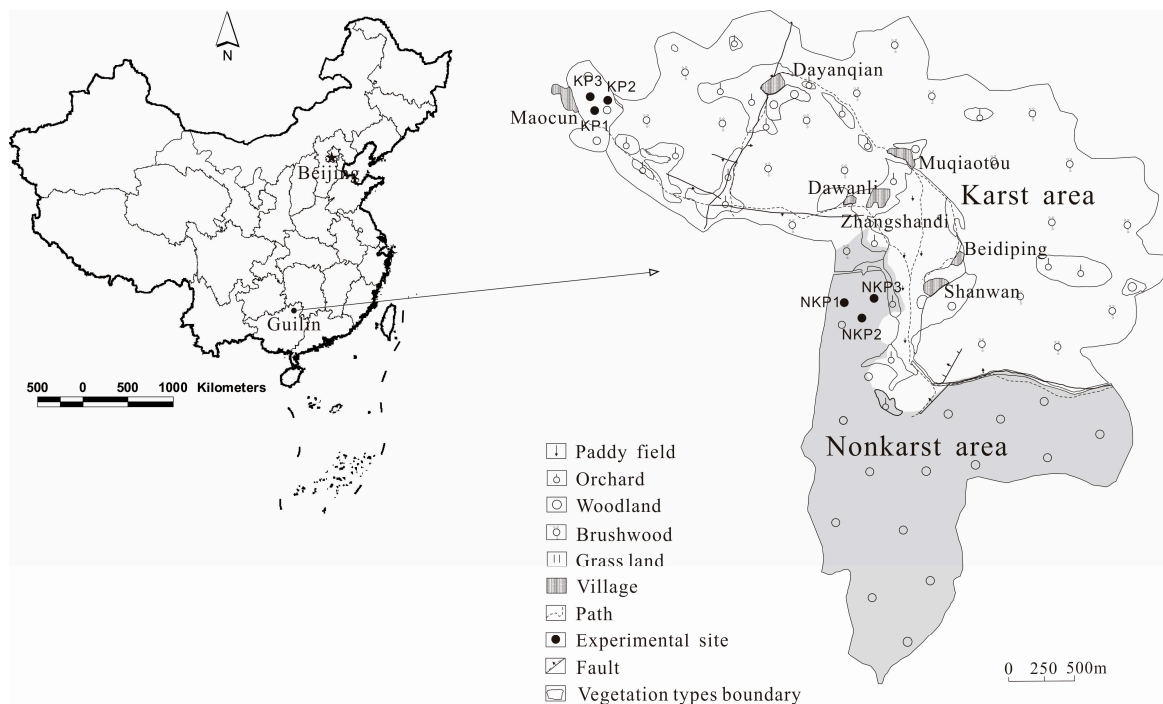


Figure 1. Land use of study area and location of study sites.

2.2. Soil Physicochemical Properties

For each layer (10, 20, 30, 40, 50, 60, 80, and 100 cm) in the 1-m deep soil profiles, we recorded water volume concentration, conductivity, and temperature using a WET sensor and HH2 moisture meter (Delta, Wakefield, UK); the corresponding range and resolutions are 0–100%, 0.1%, 0–300 mS m⁻¹, 1.0 mS m⁻¹ and –5–+50 °C, 0.1 °C. Soil pH was measured by a US IQ150 (0.00–14.00, 0.01) soil in situ acidity meter on 24 March 2015. The water volume concentration, conductivity, and temperature of the surface calcareous soil and red soil were measured monthly for one year (Table 1; Figure 2). Soil organic matter was determined by the potassium dichromate volumetric method.

Table 1. Properties at different depths in calcareous and red soils.

	Depth (cm)	pH	Organic Matter (%)	Water Content (%)	Conductivity (mS m ⁻¹)	Soil Temperature (°C)
Calcareous soil (KP1)	10	7.32	4.57 ± 0.05	26.7	92	16.3
	20	7.29	2.57 ± 0.03	22.6	106	16.4
	30	7.35	1.92 ± 0.04	23.4	112	16.1
	40	7.27	1.78 ± 0.03	22.3	115	16.1
	50	7.25	1.89 ± 0.08	22.2	118	16.0
	60	7.13	2.02 ± 0.05	20.8	123	16.0
	80	7.21	1.34 ± 0.01	26.2	117	15.8
	100	7.24	0.86 ± 0.00	32.2	116	15.7
Red soil (NKP1)	10	5.48	4.02 ± 0.03	21.9	12	17.1
	20	5.96	3.67 ± 0.05	23.3	16	16.6
	30	5.33	3.15 ± 0.05	20.3	12	16.6
	40	5.40	2.72 ± 0.03	22.0	13	16.8
	50	5.48	2.01 ± 0.08	19.5	11	17.0
	60	5.36	1.65 ± 0.00	18.1	10	17.4
	80	5.69	1.14 ± 0.01	16.2	7	17.6
	100	6.39	1.04 ± 0.06	10.7	7	17.5

Data are the mean ± standard deviation (SD). N = 3.

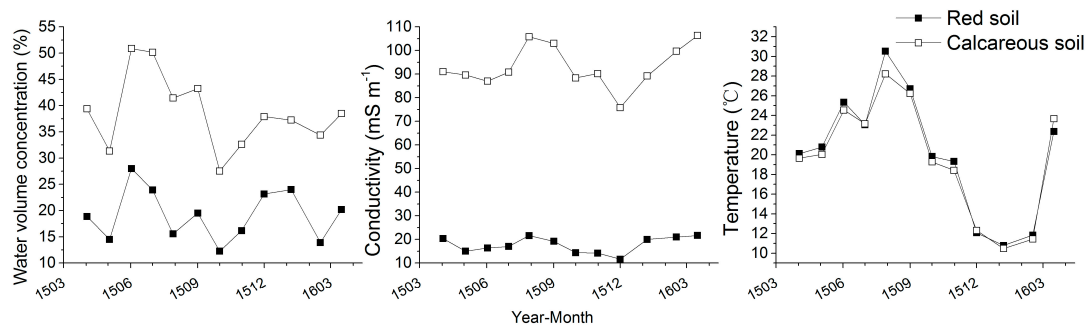


Figure 2. Temperature, water volume concentration and conductivity in the calcareous and red soils.

2.3. Soil CO₂ Concentrations and Emissions

We installed a CO₂ collection pipe in the calcareous (KP1) and red (NKP1) soil profiles in March 2015; two additional profiles in each soil type were included in January 2016 (KP2, KP3, and NKP2, NKP3), and monitoring points were separated by 5–50 m. Monthly monitoring continued from April 2015 to March 2018.

CO₂ concentrations in the eight soil layers were measured and recorded monthly (April 2015–March 2018) using a self-made soil collection pipe, comprising a 100 mL test tube in which gas was collected using a vacuum pump (GAS-TECQ Kitagawa, Japan). If CO₂ concentration >2.6%, we collected 50 mL of gas, and CO₂ concentration was doubled to give a concentration per 100 mL of gas.

Soil respiration CO₂ was collected from relatively flat ground, from which litter and weeds were removed to control for photosynthesis and the respiration of plants; the bare ground was immediately covered with a metal cylinder (25 cm diameter, 32 cm high), and the lower, open end of the cylinder was embedded 2 cm below the soil surface. A rubber tube was embedded in the soil within the cylinder and exposed to the atmosphere; a water stop clip was used to seal the end of the tube exposed to the atmosphere. Monthly atmospheric samples (April 2015–March 2018) were taken from the profiles at about 2 m above ground level to calculate background CO₂ levels; 1 h later, 200 mL of gas in the cylinder was continuously collected using a 100 mL medical syringe and injected into a vacuumed aluminum foil gas sampling bag. CO₂ concentration (ppm) was determined using an Agilent SP1 7890-0468 meteorological chromatograph (Agilent, Santa Clara, CA, USA) at the Ministry of Natural Resources/Guangxi Key Laboratory of Karst Dynamics, Guilin, Guangxi. Air pressure and temperature were simultaneously recorded. Sampling was done between 09:00 and 11:00, when soil respiration rates tend to reflect daily averages [17], to minimize diurnal variations in emissions. Soil CO₂ concentration and respiration in KP1 and NKP1 were sampled 33 times, and 23 times from the remaining profiles.

The δ¹³C-CO₂ was measured from the eight layers in the soil profiles in June and December 2015, and July 2017, where we used a vacuum to extract soil CO₂ into sealed aluminum bags. The δ¹³C-CO₂ analysis was completed at the isotope laboratory of the Chinese Academy of Agricultural Sciences, Beijing, China using a MAT253 mass spectrometer. Samples were collected from KP1 and NKP1 three times, and once from the remaining profiles.

2.4. Dissolution Rate of Carbonate Rock

The rate was acquired through the standard carbonate tablet method [18]. Carbonate tablets were determined from high purity, 4 cm diameter × 0.3 cm thick calcareous tablets that were washed and subsequently dried at 70 °C to constant weight after cooling, through a repeated dry-weight process. In March 2015, in KP1 and NKP1, three tablets were placed 150 cm above the ground, at the soil surface, and inserted at the 20, 50, and 100 cm soil layers. In June, September, and December 2015, and March 2016, the tablets were recovered, analyzed, and re-buried following the washing and drying process described above.

2.5. Data Analysis

The units of CO₂ measurement (ppm) were converted to mg m⁻³ using:

$$\text{CO}_2 = \frac{M}{22.4} \times \text{ppm} \times \frac{273}{273 + T} \times \frac{\text{Ba}}{101325} \quad (1)$$

where M is the molecular weight of the gas; ppm is the measured volume concentration; T is the atmospheric temperature (°C); and, Ba is atmospheric pressure (Pa).

Soil respiration rate (V_R ; mg C m⁻² h⁻¹) was calculated as:

$$V_R = \frac{(C_1 - C_0) \times V}{S \times h} \times \frac{12}{44} \quad (2)$$

where C_1 is CO₂ concentration in the cylinder (mg m⁻³); C_0 is the corresponding background CO₂ concentration (mg m⁻³); V is the sampling box volume (m³); S is the area of sampled soil (m²); and, h is the monitoring time (h).

Annual soil CO₂ emission flux (F; t C km⁻² a⁻¹) was calculated as:

$$F = \frac{\sum_{i=1}^n V_n \times (T_n - T_{n-1}) \times 24 \times 10^{-3}}{\frac{(T_n - T_1)}{365}} \quad (3)$$

where V_n is the nth measured soil respiration rate (mg C m⁻² h⁻¹); $T_n - T_{n-1}$ and $T_n - T_1$ are the nth and (n-1)th, the nth and 1st sampling intervals (d), respectively.

The annual dissolution rate of the carbonate tablet (ER; mg cm⁻² a⁻¹) was calculated as:

$$\text{ER} = (W_1 - W_2) \times 1000 \times \frac{T}{365 \times S} \quad (4)$$

where W_1 is the initial weight of the tablet (g); W_2 is the weight after embedding (g); T is the embedding duration (d); and S is the tablet surface area (about 28.9 cm²).

CO₂ recovery in calcareous soil (CR_C ; t C km⁻² a⁻¹) was calculated according to the stoichiometric coefficient ratio of the carbonate dissolution reaction:



$$\text{CR}_C = \text{ER} \times 97\% \times \frac{12}{100} \times 10 \quad (6)$$

where ER is the annual dissolution rate of the carbonate tablet (mg cm⁻² a⁻¹); 97% is the purity of the standard carbonate tablet.

The dissolution rate of carbonate rocks in calcareous soil is 23.8 times that of clastic rocks in red soil at the study site [19]. According to the clastic rock dissolution reaction:



the CO₂ recovery in red soil (CR_R ; t C km⁻² a⁻¹) was calculated this way:

$$\text{CR}_R = \frac{\text{CR}_C}{23.8} \times 2 \quad (8)$$

We used one-way analysis of variance (ANOVA) to analyze the differences in soil respiration rate, CO₂ concentration, and $\delta^{13}\text{C}$ -CO₂ among the soil layers between the two soil types at $p = 0.05$. A Pearson correlation analysis was used to test for association between CO₂ concentration and $\delta^{13}\text{C}$ -CO₂ in different layers. Analyses were performed in Statistical Package Social Science (SPSS ver. 20.0; IBM Corp., Armonk, NY, USA).

3. Results

3.1. Soil Respiration Rate and Flux

There was a single peak in the soil respiration rate in one year of the karst and non-karst soil profiles, and soil respiration rates varied among the three calcareous soil profiles (range: 9.02–437.33 mg C m⁻² h⁻¹, average: 134.84 mg C m⁻² h⁻¹), where they were greater in KP2 than KP1; there were no differences among the red soil profiles (range: 23.21–361.42 mg C m⁻² h⁻¹, average: 137.93 mg C m⁻² h⁻¹) (Figure 3). No difference in the mean soil respiration rate was found between the two soil types, but the variation was greater in calcareous soil. The average CO₂ emission flux in calcareous soil and red soil was 1305 and 1167 t C km⁻² a⁻² (Table S1), being 12% higher in calcareous soil.

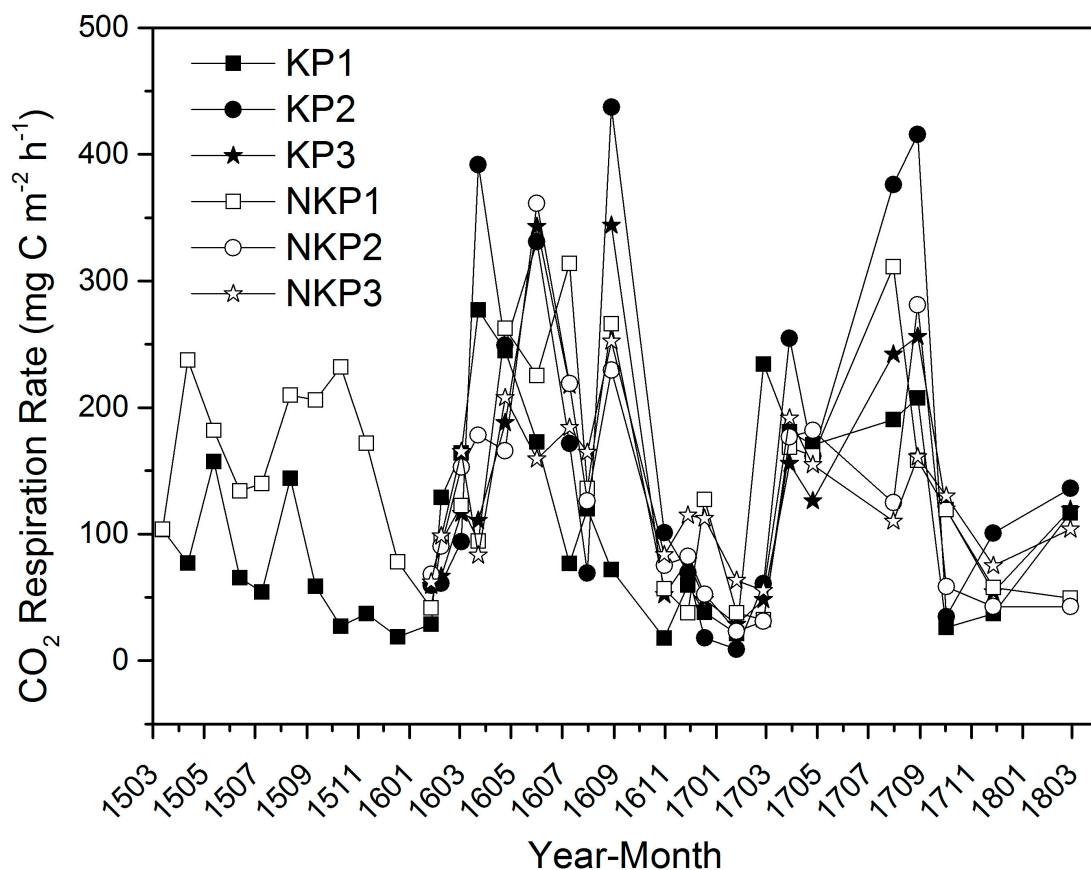


Figure 3. Respiration rates in the calcareous and red soils.

3.2. Variation in CO₂ Concentration among Soil Layers

Consistent with changes in soil respiration rate, the seasonal variation in soil CO₂ concentration in the layers tended to be unimodal, and concentrations were universally greater in summer and autumn than in winter and spring; an anomaly was the low value recorded in July 2015 and August 2016 (Figure 4). Overall, CO₂ concentrations were greatest and most variable in KP2, and lowest in KP1. There were no differences in CO₂ concentrations among the three red profiles.

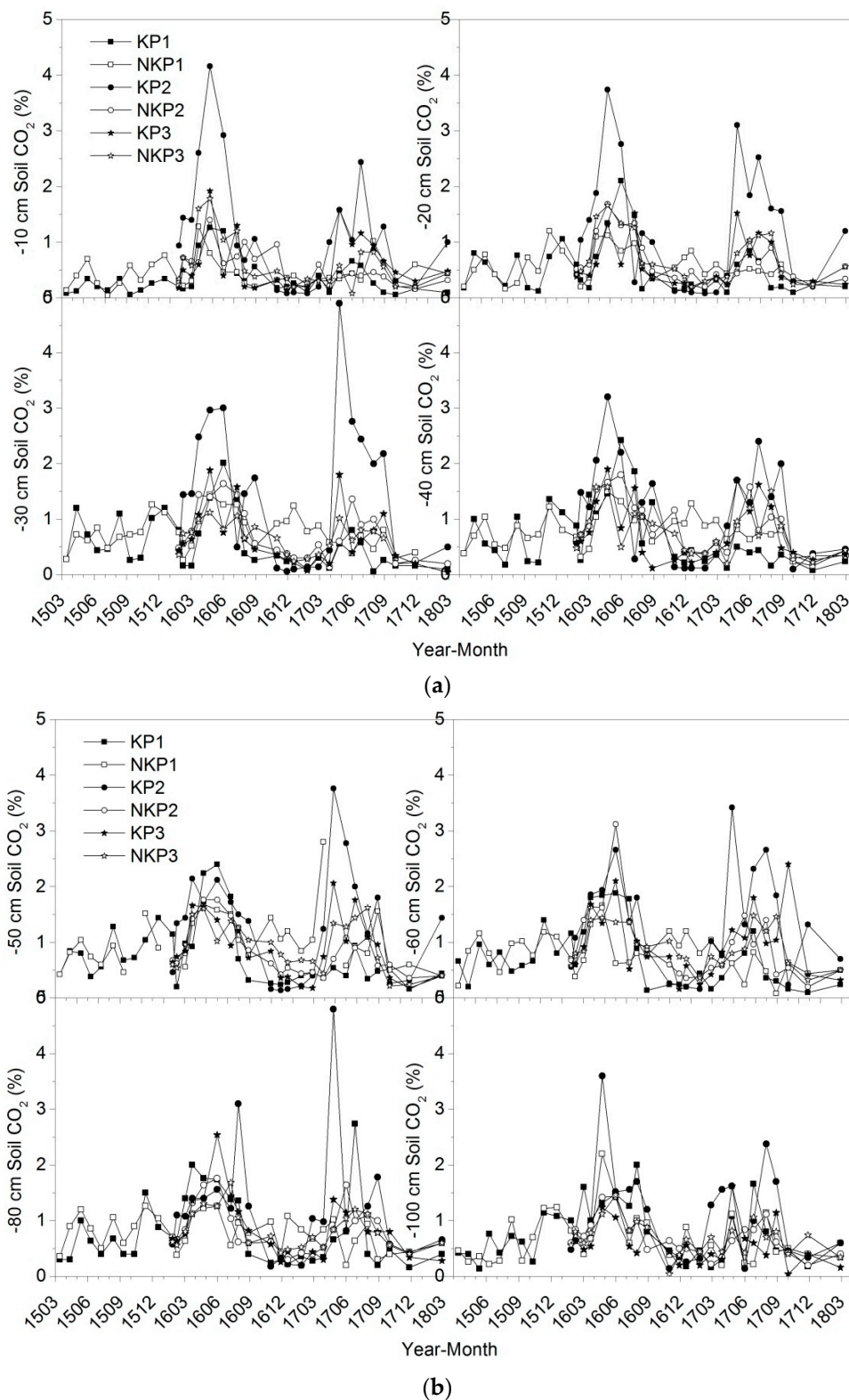


Figure 4. Soil CO₂ concentrations at 10–40 cm (a) and 50–100 cm (b) depths in calcareous and red soils.

Soil CO₂ concentration in the calcareous soil and red soil profiles varied with depth, where it tended to be higher at 50–60 cm and lower in the upper and deeper layers; this pattern was clearer in the red soils (Figure 5). The mean CO₂ concentrations in the three calcareous soils were 11% greater than in the red soils (Table S2).

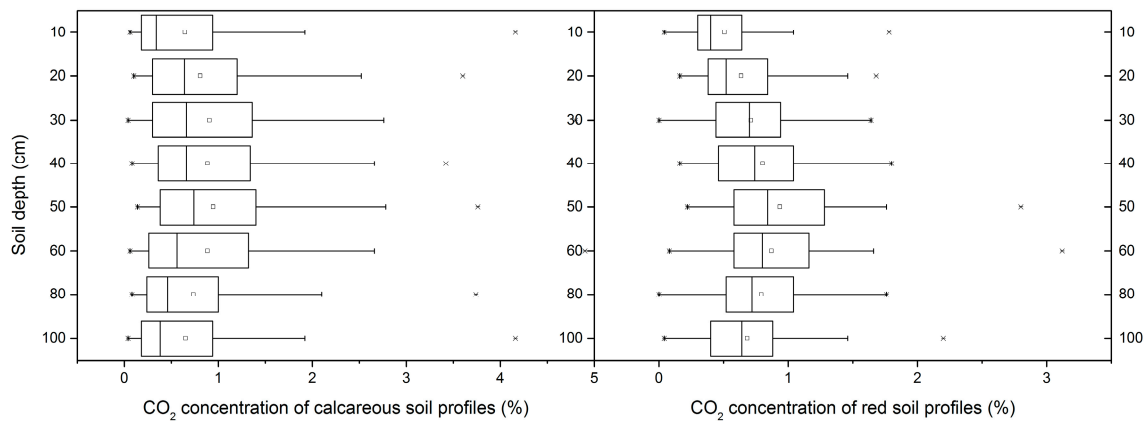


Figure 5. Summary statistics of overall mean soil CO₂ concentrations in calcareous and red soils. Open square: average; vertical line: median; box: upper and lower quartiles; horizontal lines: 1st and 99th percentiles; x: minimum and maximum values. N = 168.

3.3. Changes in $\delta^{13}\text{C-CO}_2$ among Soil Layers

In the calcareous soils, there was a bidirectional gradient of $\delta^{13}\text{C-CO}_2$ with a depth in KP1 and KP3, and values at 60 cm were lighter than those of either the upper or deeper layers; the $\delta^{13}\text{C-CO}_2$ values were lightest in KP2 and heaviest in KP1, with respective averages of -26.28‰ and -24.24‰ (Figure 6). In the red soils, $\delta^{13}\text{C-CO}_2$ decreased with a depth of up to 50 cm, but it remained stable from 50 cm to 100 cm. The mean value of three plots for all layers was 0.87‰ heavier in calcareous soil than red soil (Table S3).

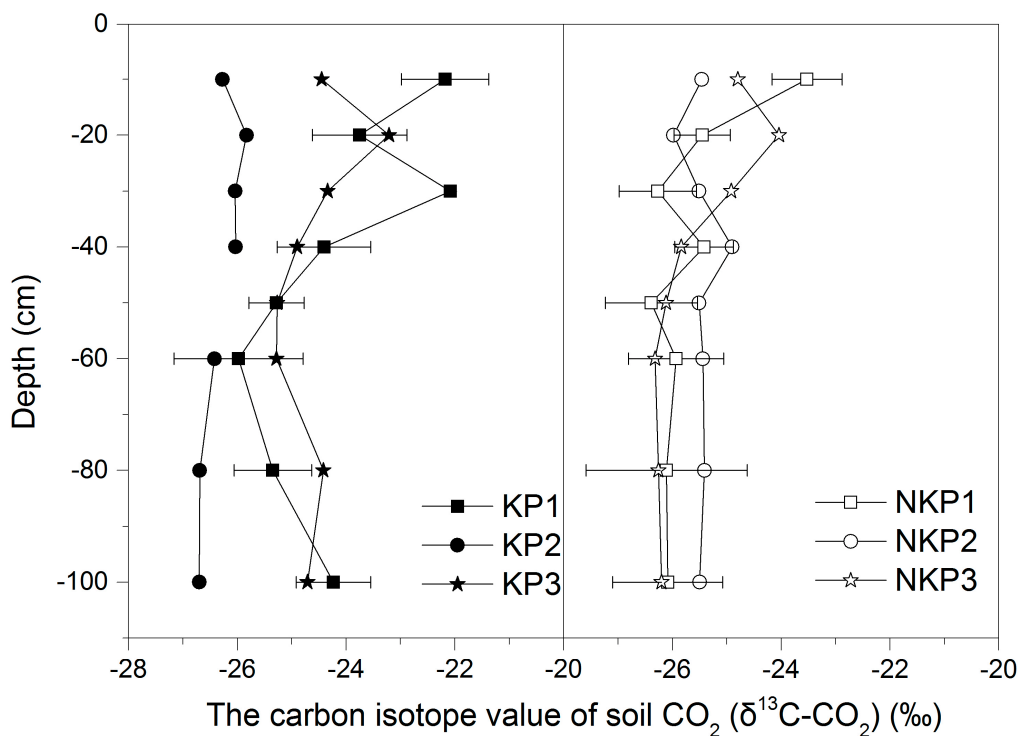


Figure 6. $\delta^{13}\text{C-CO}_2$ values in different depth layers of the calcareous and red soils.

3.4. Dissolution Rates of the Carbonate Tablets in Different Layers

The dissolution rates of carbonate tablets were greater in the two soil types than in the air above the profiles, and their rates were greatest in the summer (Figure 7). The rates were bidirectional with

increasing depth and were greater in red soil than calcareous soil, except in calcareous soil during summer. There was no difference in the mean rates in the air above the calcareous and red soils, with averages of 2.50 ± 0.91 and $2.03 \pm 1.07 \text{ mg cm}^{-2} \text{ a}^{-1}$, respectively. The corresponding rates in the soil were 7.20 ± 2.11 and $13.88 \pm 5.42 \text{ mg cm}^{-2} \text{ a}^{-1}$, being 48% lower in calcareous soil (Table S4).

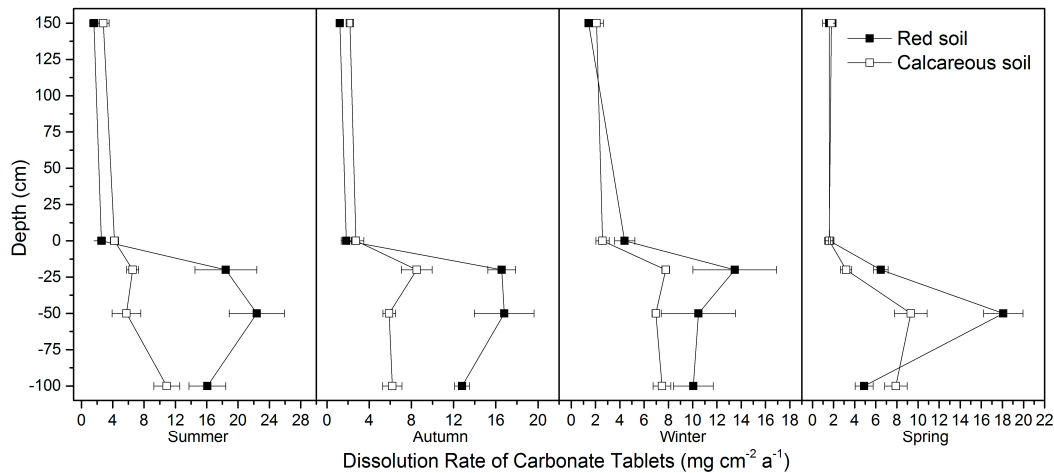


Figure 7. Dissolution rates in calcareous and red soils.

4. Discussion

4.1. Bidirectional Gradient of Soil CO_2 Concentrations and CO_2 Emissions in Red and Calcareous Soil Profile

Wang [13] and Dai [14] found that soil concentrations of CO_2 increased with a greater depth (up to 50 cm) but then diminished below 60 cm, due to the low associated organic carbon content. In our study, soil CO_2 concentrations in the two soil types had a bidirectional gradient trend, though this was more pronounced in the red soil, where the maximum values were recorded in the 50–60 cm layer. Soil organic matter (SOM) on the surface of calcareous soil was clearly higher than that of red soil (Table 1), but it exhibited the opposite trend deeper in the profile. Additionally, there is only a single trend of a gradually decreasing SOM content in red soil, while calcareous soil has a tendency to increase slightly at 50–60 cm. Therefore, the distribution of SOM should be a major reason why the concentration of CO_2 in deep layers of red soil decreases faster than in calcareous soil.

Our experiment showed that the diffusion input of atmospheric CO_2 was greater until the 50–60 cm layer, indicating that the thickness of the soil–atmosphere interface layer was 50–60 cm, while soil CO_2 in deeper layers was probably controlled by oxidative decomposition of organic matter. It is likely that the physical structure of soil particles and porosity, clay content, and soil flooding may also affect the thickness of the soil–atmosphere interface layer [20–22].

The annual soil respiration flux varies greatly in southwest China, ranging from $4.5 \text{ t C ha}^{-1} \text{ a}^{-1}$ ($450 \text{ t C km}^{-2} \text{ a}^{-1}$) in Yaji, Guilin, Guangxi, to $150 \text{ mg C m}^{-2} \text{ h}^{-1}$ ($1314 \text{ t C km}^{-2} \text{ a}^{-1}$) in Qingmuguan, Chongqing [9,23–25]. The results of our study are close to the largest value in those studies. The results were four to six times greater than those of typical meadow and dryland systems in a temperate continental monsoon climate zone ($2.8\text{--}4.8 \text{ t C ha}^{-1} \text{ a}^{-1} = 280\text{--}480 \text{ t C km}^{-2} \text{ a}^{-1}$) [22], perhaps due to lower temperatures in the temperate zone. Soil temperature, which is a key driver of soil respiration, is exponentially related to soil CO_2 [26].

Soil moisture also drives the soil respiration rate, and directly and indirectly regulates soil CO_2 emissions. It is believed that soil respiration increases with increasing soil moisture, until it reaches a threshold, after which it declines [20]. For example, when soil moisture is $>60\%$ in shallow soil, CO_2 flux rapidly decreases, due to the restriction of gas transport by the moisture [21], and a soil water content of 25–45% is optimal for microbe activity [27]. Soil moisture in the profile of calcareous soil was horizontally and vertically higher than that of the profile of red soil (Table 1, Figure 2), which may

have been responsible for the higher CO₂ concentration and respiration characterizing the calcareous soil profile.

4.2. Soil CO₂ Concentration and δ¹³C-CO₂ Affected by Karstification

Consistent with our results, the CO₂ produced in soil had a lighter mean δ¹³C value of $-21 \pm 1.5\text{‰}$ than CO₂ with heavier isotopes in the surface atmosphere did (-9.82‰) [15], indicating a greater exchange of soil and air CO₂ at the soil–atmosphere interface. Therefore, δ¹³C-CO₂ from the soil–atmosphere interface layer and upward gradually becomes heavier.

We found heavier δ¹³C-CO₂ in the calcareous karst soils below 50–60 cm, due to two possible reasons. Firstly, karstification consumes soil CO₂, and lighter C is moved downward; the nearer the bedrock, the greater the likelihood of consumption of lighter C, resulting in heavier δ¹³C-CO₂ in the soil. Secondly, the δ¹³C of the rock is 0‰, and the theoretical CO₂ isotope value for bicarbonate formed by karstification at the soil–rock interface dissociation into soil CO₂ is -14‰ [28]; therefore, lighter δ¹³C-CO₂ derived from root respiration, soil organic matter oxidative decomposition, and soil microbe activity could be mixed with this part of CO₂, resulting in a decreased overall CO₂ isotope value.

The δ¹³C-CO₂ in the red soil below 50–60 cm tended to be stable; this finding is consistent with other studies in non-karst areas [29]. This stability with increasing soil depth may be attributed to the composition of stable carbon isotopes of CO₂ produced from the soil or the limited impacts of the climate on the physical properties of deep soils. The lightest value of soil CO₂ occurred at 50–60 cm, both in calcareous and red soils, which further corroborated that the 50–60 cm layer was the bottom of the soil–atmosphere interface layer.

Below the soil–atmosphere interface layer, karstification at the soil–rock interface consumes CO₂ and drives the downward migration of CO₂ [9]. This process may also have caused slow declines in CO₂ concentration at the bottom profile of the calcareous soil, resulting in a less pronounced bidirectional gradient than in the red soil profile. The δ¹³C-CO₂ in calcareous soil became heavier: both the CO₂ concentration and its isotopes of calcareous soil show a bidirectional gradient due to the contribution from karstification, so a significant positive correlation arose between the CO₂ concentration and its isotopes (Figure 8). However, this was not the case in the red soil profile.

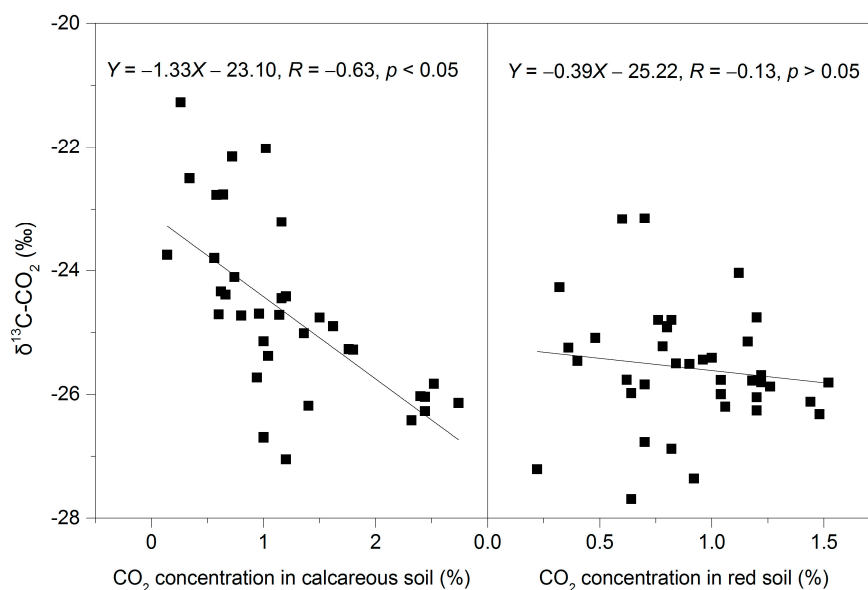


Figure 8. Association between δ¹³C-CO₂ and the CO₂ concentration in calcareous and red soils.

4.3. Source–Sink Effect of Karst Soil Carbon Pools

In this study, the dissolution rate of the carbonate tablet in the red soil was found to be 1.93 times that of the calcareous soil (Table 2); however, soil CO₂ concentration and soil respiration rates were not as high (1.16 and 1.42 times, respectively, for NKP1 versus KP1), possibly due to a lower soil pH in the red soil affecting the rate of soil organic matter decomposition and erosion by soil microorganisms [30].

Table 2. The ratio of CO₂ recovery to CO₂ emission in calcareous soil and red soil.

	Calcareous Soil	Red Soil
Carbonate dissolution rate in air (mg cm ⁻² a ⁻¹)	2.50	2.03
Carbonate dissolution rate in soil (mg cm ⁻² a ⁻¹)	7.20	13.88
CO ₂ recovery (t C km ⁻² a ⁻¹)	8.38	0.70
Soil CO ₂ emission flux (t C km ⁻² a ⁻¹)	1305	1167
CO ₂ recovery/CO ₂ emission (%)	0.64	0.06

Influenced by soil temperature, water, soil CO₂, soil organic matter and pH, in addition to soil pores and other conditions [31], the dissolution rate of carbonate tablets in the soil in forests in karst areas in southwest China vary widely, ranging from 1.99 mg cm⁻² a⁻¹ in Yaji, Guilin, Guangxi [24], to 357.93 mg m⁻² d⁻¹ (13.06 mg cm⁻² a⁻¹) in Dalongdong, Hunan [32]. The corresponding value obtained in our study is in the middle of these (Table 2), which can be considered as a better representative. The dissolution rate of carbonate tablets in the air is mainly controlled by the concentration of atmospheric CO₂ and rainfall intensity [18], and the difference between the data in this study (Table 2) and that from Jinfo Mountain, Chongqing, (21.4 t km⁻² a⁻¹ = 2.14 mg cm⁻² a⁻¹) [18] is not large.

According to Table 2, CO₂ recovery accounts for 0.64% of the soil carbon source for calcareous soil. It is clear, then, that although karstification is an active weathering process, decomposition of soil organic matter and associated CO₂ respiratory emissions dominate the transport and cycling of carbon in the soil system. Thus, karstification and its impact on the carbon cycle represent an Earth-surface carbon transfer process.

Although the carbon source of calcareous soil was 1.12 times that of red soil, its carbon sink effect is 11.97 times that of red soil, suggesting that karst soil contributes greatly to the reduction of atmospheric CO₂. Nonetheless, the dissolution rate of carbonate tablets in the air could be indicative of the carbonate rock dissolution rate in bare karst areas, which is only 0.35 times that of calcareous soil. However, due to the wide distribution of bare karst in southwest China, its carbon sink potentiality cannot be ignored. The high carbonate dissolution rate in red soil also indicated the huge carbon sink potential of zonal red soil-intercalated carbonate rocks.

5. Conclusions

The CO₂ concentrations in calcareous and red soil layers exhibited bidirectional responses to soil depth. The influence of the soil–atmosphere interface on CO₂ exchange extended to a depth of 50–60 cm, where CO₂ concentration increased with depth; below this, CO₂ concentration decreases with depth and is mainly controlled by organic matter decomposition.

Soil δ¹³C-CO₂ in the two soils was controlled by CO₂ exchange at the soil–atmosphere interface and downward—where isotopes become lighter with depths of 50–60 cm; beyond this, δ¹³C-CO₂ gradually became heavier in calcareous soil layers, being mainly controlled by karstification. The CO₂ in the red clastic soils was derived from organic matter with stable isotopes, and so δ¹³C-CO₂ values were stable at depths >50–60 cm. The overall average of δ¹³C-CO₂ was 0.87‰ heavier in calcareous soils than red soils.

There were also bidirectional differences evident in the dissolution rates of carbonate rock in the two contrasting soils. The rates in the calcareous soil and red soil were 7.20 ± 2.11 and 13.88 ± 5.42 mg cm⁻² a⁻¹, and, thus, almost half as low (48% lower) in calcareous soil.

Although karstification is an active weathering process, the decomposition of soil organic matter and associated CO₂ respiratory emissions dominate the transport and cycling of carbon in the system. The soil carbon sink only accounts for 0.64% of carbon sources in the karst areas. However, the CO₂ recovery in karst soil is estimated to be 11.97 times that of the clastic rock area and 1.12 times the latter as a carbon source, indicating the key role of karst soil in reducing atmospheric CO₂.

Supplementary Materials: The following are available online at <http://www.mdpi.com/1999-4907/11/2/219/s1>, Figure S1: Temperature and rainfall in Maocun village, Table S1: Respiration rates in calcareous and red soils, Table S2: CO₂ Concentrations in different layers in calcareous and red soils, Table S3: δ¹³C-CO₂ values at different depths of calcareous and red soils, Table S4: Seasonal carbonate dissolution rates in calcareous and red soils.

Author Contributions: Conceptualization, J.C.; writing—original draft preparation, F.H.; investigation, M.R. and M.F., writing—review and editing, J.C. and T.Z. All authors have read and agreed to the published version of the manuscript.

Funding: This study was supported by the National and Guangxi Natural Science Foundation of China (Grant Nos. 41772385, 2016GXNSFAA380034, 41530316), the National Key Research Projects (Grant No. 2016YFC05025), and the China Geological Survey (Grant No. DD20160305).

Acknowledgments: Special thanks go to the anonymous referees for their valuable comments and suggestions.

Conflicts of Interest: The authors declare no conflict of interest.

References

1. Jobbagy, E.G.; Jackson, R. The Vertical Distribution of Soil Organic Carbon and Its Relation to Climate and Vegetation. *Ecol. Appl.* **2000**, *10*, 423–436. [CrossRef]
2. Sheng, H.; Yang, Y.S.; Yang, Z.J.; Chen, G.S.; Xie, J.S.; Guo, J.F.; Zou, S.Q. The dynamic response of soil respiration to land-use changes in subtropical China. *Glob. Chang. Biol.* **2010**, *16*, 1107–1121. [CrossRef]
3. Ben, B.L.; Allison, T. Temperature-associated increases in the global soil respiration record. *Nature* **2010**, *464*, 579–582.
4. Cao, J.; Yang, H.; Kang, Z. Preliminary regional estimation of carbon sink flux by carbonate rock corrosion: A case study of the Pearl River Basin. *Chin. Sci. Bull.* **2011**, *56*, 3766–3773. [CrossRef]
5. Li, D.; Luo, Y. Measurement of carbonate rocks distribution area in China. *Carsologica Sin.* **1983**, *2*, 147–150. (In Chinese)
6. Liu, Z.; Wolfgang, D. Comparison of carbon sequestration capacity between carbonate weathering and forests: The necessity to change traditional ideas and methods of study of carbon sinks. *Carsologica Sin.* **2012**, *31*, 345–348. (In Chinese)
7. Fang, J.; Guo, Z.; Piao, S.; Chen, A. Estimation of terrestrial vegetation carbon sink in China from 1981 to 2000. *Sci. China Ser. D* **2007**, *37*, 804–812. (In Chinese)
8. Huang, Q.; Qin, X.; Liu, P.; Zhang, L.; SU, C. Proportion of pedogenic carbonates and the impact on carbon sink calculation in karst area with semiarid environment. *Carsologica Sin.* **2016**, *35*, 164–172. (In Chinese)
9. Cao, J.; Zhou, L.; Yang, H.; Lu, Q.; Kang, Z. Comparison of carbon transfer between forest soils in karst and clasolite areas and the karst carbon sink effect in Maocun village of Guilin. *Quat. Sci.* **2011**, *31*, 431–437. (In Chinese)
10. He, S.; Zhang, M.; Xu, S. Observation on soil CO₂ concentration, hydrochemistry, and thier relationship with karst processes. *Carsologica Sin.* **1997**, *16*, 319–324.
11. Xu, S.; He, S. The CO₂ regime of soil profile and its drive to dissolution of carbonbate rock. *Carsologica Sin.* **1996**, *15*, 50–57. (In Chinese)
12. Li, T.; Wang, S.; Zheng, L. Comparative study on sources of CO₂ from overlying carbonate rocks and non-carbonate rocks, in the middle parts of Guizhou province. *Sci. China Ser. D* **2001**, *31*, 777–782. (In Chinese)
13. Wang, C.; Huang, Q.; Yang, Z.; Huang, R.; Chen, G. Analysis of vertical profiles of soil CO₂ efflux in Chinese fir plantation. *Acta Ecol. Sin.* **2011**, *31*, 5711–5719. (In Chinese)
14. Dai, W.; Wang, Y.; Huang, Y.; Liu, J.; Zhao, L. Seasonal dynamic of CO₂ concentration in lou soil and impact by environmental factors. *Acta Pedol. Sin.* **2004**, *41*, 827–831. (In Chinese)
15. Zheng, L. The stable carbon isotope composition of soil CO₂ in the karst areas, the middle parts of Guizhou province. *Sci. Chin. Ser. D* **1999**, *29*, 514–519. (In Chinese)

16. Huang, C. *Soil Science*; China Agriculture Press: Beijing, China, 2000; pp. 224–227. (In Chinese)
17. Bubier, J.; Crill, P.; Mosedale, A.; Frolking, S.; Linder, E. Peatland responses to varying interannual moisture conditions as measured by automatic CO₂ chambers. *Glob. Biogeochem. Cycles* **2003**, *17*. [[CrossRef](#)]
18. Zhang, C. Carbonate rock dissolution rates in different landuses and their carbon sink effect. *Chin. Sci. Bull.* **2011**, *56*, 2174–2180. [[CrossRef](#)]
19. Huang, F.; Zhang, C.L.; Xie, Y.C.; Li, L.; Cao, J.H. Inorganic carbon flux and its source in the karst catchment of Maocun, Guilin, China. *Environ. Earth Sci.* **2015**, *74*, 1079–1089. [[CrossRef](#)]
20. Gong, X.; Li, Y.; Wang, X.; Niu, Y.; Lian, J.; Luo, Y. Characteristics of soil CO₂ emission in relation to hydrothermal factors during the growing season in horqin sandy land. *Ecol. Environ.* **2018**, *27*, 634–642. (In Chinese)
21. Gabriel, C.E.; Kellman, L. Investigating the role of moisture as an environmental constraint in the decomposition of shallow and deep mineral soil organic matter of a temperate coniferous soil. *Soil Biol. Biochem.* **2014**, *68*, 373–384. [[CrossRef](#)]
22. Jiang, C.; Hao, Q.; Song, C.; Hu, B. Effects of marsh reclamation on soil respiration in the Sanjiang Plain. *Acta Ecol. Sin.* **2010**, *30*, 4539–4548. (In Chinese)
23. Wu, X.; Pan, M.; Zhu, X.; Zhang, M.; Bai, X.; Zhang, B. Precipitation effect on soil respiration in epikarst during summer. *J. South. Agric.* **2015**, *46*, 575–580. (In Chinese)
24. Pan, G.; He, S.; Cao, J.; Tao, Y.; Sun, Y. Variation of δ¹³C value in karst soil system in the surface zone of Yaji Village, Guilin. *Chin. Sci. Bull.* **2001**, *46*, 1919–1922. (In Chinese)
25. Li, L.; Xian, H.; Kuang, M.; Xie, S.; Zhang, Y.; Jiang, Y.; Liu, Y. The regularity of CO₂ release from soils of the epikarst ecosystem in the Jinfu mountain, Chongqing. *Acta Geosci. Sin.* **2006**, *27*, 329–334. (In Chinese)
26. Wang, X.; Wang, X.; Han, G.; Wang, J.; Song, W.; You, Z. Dynamics of soil CO₂ concentration and CO₂ efflux in non-growing season of the Yellow River Delta wetland. *Chin. J. Ecol.* **2018**, *37*, 2698–2706.
27. Schindlbacher, A.; Zechmeister-Boltenstern, S.; Kitzler, B.; Jandl, R. Experimental forest soil warming: Response of autotrophic and heterotrophic soil respiration to a short-term 10 °C temperature rise. *Plant Soil* **2008**, *303*, 323–330. [[CrossRef](#)]
28. Jiang, Y.J. The contribution of human activities to dissolved inorganic carbon fluxes in a karst underground river system: Evidence from major elements and delta δ¹³C_{DIC} Nandong, Southwest China. *J. Contam. Hydrol.* **2013**, *152*, 1–11. [[CrossRef](#)]
29. Ding, P.; Shen, C.; Wang, N.; Yi, W.; Ding, X.; Fu, D.; Liu, K.; Zhao, P. Carbon isotopic composition turnover and origins of soil of soil CO₂ in a monsoon evergreen broad leaf forest in Dinghushan Biosphere Reservior, South China. *Chin. Sci. Bull.* **2010**, *55*, 779–787. (In Chinese) [[CrossRef](#)]
30. Zhao, R.; Lv, X.; Jiang, J.; Duan, Y. Factors affecting soil CO₂ and karst carbon cycle. *Acta Ecol. Sin.* **2015**, *35*, 4257–4264. (In Chinese)
31. Liu, W.; Zhang, Q.; Jia, Y. The influence of meteorological factors and soil physicochemical properties on karst processes in six land-use patterns in summer and winter in a typical karst valley. *Acta Ecol. Sin.* **2014**, *34*, 1418–1428. (In Chinese)
32. Wang, W.; Lan, F.; Jiang, Z.; Qin, X.; Lao, W. Corrosion rate of carbonate tablet under diverse land use and lithology in the Dalongdong basin, Hunan. *Carsologica Sin.* **2013**, *32*, 29–33. (In Chinese)

